A feasibility study for a low energy threshold particle detector in a xenon crystal

Prepared for submission to JINST

15TH Topical seminar on innovative particle and radiation detectors
14-17 October 2019
Siena

A feasibility study for a low energy threshold particle detector in a xenon crystal

M. Guarise,[a,1] **C. Braggio,**[b] **R. Calabrese,**[a] **G. Carugno,**[b] **A. Dainelli,**[c] **A. Khanbekyan,**[a] **E. Luppi,**[a] **E. Mariotti,**[d] **and L. Tomassetti**[a]

[a] *Dipartimento di Fisica e Scienze delle Terra, Università di Ferrara and INFN Fe*
Via G. Saragat 1, 44122 Ferrara Italy
[b] *Dipartimento di Fisica e Astronomia, Università di Padova and INFN Pd*
Via F. Marzolo 8, 35100 Padova Italy
[c] *Laboratori Nazionali di Legnaro INFN*
Viale dell'università 1, 35020 Legnaro Italy
[d] *Dipartimento di Scienze Fisiche, della Terra e dell'Ambiente, Università di Siena and INFN Pi*
Via Roma 56, 53100 Siena Italy

E-mail: marco.guarise@unife.it

Abstract: In this paper we report on the growing of a large xenon crystal that can be used as low energy threshold particle detector for applications in dark matter searches. A large xenon crystal of $\sim 150\,\mathrm{cm}^3$ volume has been grown exploiting the Bridgman-Stockbarger modified technique in a pyrex chamber. The crystal has been used as a proof of concept of the proposed detection scheme as a sensor for cosmic rays.

Keywords: Dark matter detectors (WIMPs, axions, etc.); Charge transport and multiplication in solid media; Noble liquid detectors (scintillation, ionization, double-phase); Cryogenic detectors

[1] Corresponding author.

Contents

1 Introduction

1.1 Dark matter: proofs and candidates

From experimental observations on all astrophysical and cosmological scales, an outstanding result is that there is something in the Universe which is not visible but has a gravitational effect. Historically this hidden part of the Universe is called dark matter (DM) because it does not absorb or emit any electromagnetic radiation but it interacts only through the gravitational force and, likely, the weak force. Many evidences for the existence of dark matter, all based on the gravitational interaction, have been provided in the previous decades. The rotation curve of galaxies, the gravitational lensing effect, the galaxy clustering, the object 1E 0657-558 also named Bullet Cluster which is the collision of two galaxy clusters, the Cosmic Microwave Background anisotropies, among others, are the main evidences for the existence of non visible matter. Furthermore it is also possible to estimate that more than around 80% of the Universe mass is composed by dark matter, while only less than 20% is made of ordinary matter [1, 2].

A possible solution to the DM problem can be found introducing big massive galactic objects such as MACHOs (massive compact halo objects), but unsuccessful searches for these objects in the dark halo of our galaxy ruled out this possibility and also give an upper limit to the mass of DM candidates: $m_{max} \leq 2 \cdot 10^{-9} M_{\odot} \approx 2 \cdot 10^{48}\,\mathrm{GeV/c^2}$. This limit and the lack of other candidates besides primordial black holes, constitute the observational arguments we have in favor of elementary particles as DM candidates [3–5].

Besides supersimmetric particles, especially s-neutrinos and gravitinos, whose existence can be probed in high-energy accelerators, axions and WIMPs are ones of the favoured DM candidates. The axion is a particle introduced by R. Peccei and H. Quinn in the '70s to solve the strong charge conjugation parity (CP) problem of the Standard Model, i.e. the absence of CP symmetry violation in the strong interaction [6]. Axions and also axion-like-particles are one of the lightest candidates for the solution of the dark matter problem. The generic class of particles known as Weakly Interacting Massive Particles (WIMPs) are non-baryonic particles with no charge and color, and they can only interact through the gravitational and the weak force. These heavy particles represent a possible solution of the DM problem in a scenario of physics beyond the Standard Model [7].

1.2 DM detectors: state of the art

Starting from DM proposal, many experiments have been devised to search for the existence of elementary DM candidates. The principal requirements for DM detectors are the low background and the large volume which is necessary to maximize the interaction probability. Furthermore, since the mass range of DM candidates can extend below the eV, a low energy threshold is also an important requirement.

Besides some ad hoc schemes, such as direct conversion of DM particles into visible ones, the standard detection techniques can be roughly summarized into three large categories, depending on the signal they exploit [8]: scintillators, ionization detectors and bolometers. The best lower limit for the WIMP-nucleon interaction cross section is currently given by $\sigma_{\mathrm{WIMP-Xe}} = 4.1 \cdot 10^{-47}\,\mathrm{cm}^2$ at $m_{\mathrm{WIMP}} = 30\,\mathrm{GeV/c}^2$, obtained by the XENON1T collaboration in a science run last year [9].

2 The proposed detection scheme in undoped rare gas crystals

We propose to exploit rare gases (RG) in the solid phase as active materials for a novel kind of particle detector that exploits the electrons' extraction from these solids combined with the in-vacuum single-electron detection.

2.1 Rare cas properties

The family of RG, also known as noble or inert gases, comprises the six elements of the VIII group of the periodic table. They are: helium (He), neon (Ne), argon (Ar), kripton (Kr), xenon (Xe) and radon (Rn). The atoms of this group have a stable electronic configuration in the form $1s^2$ or ns^2np^6. This implies that their outer shell of valence electrons is completely "full", making them highly unreactive except under particular extreme conditions. Rare gases have been used in the last four decades as active media for particle detectors, especially in the gas and liquid phases, due to their very exclusive combination of properties such as the energy gap, the light yield and the electron mobility. Furthermore, observations regarding the electron mobility indicate that it should increase lowering the temperature. Table 1 shows some important features of RG.

At room temperature, rare gas atoms do not form stable chemical bonds between them. At standard temperature and pressure conditions all the rare gases are indeed in the gaseous state, and crystallization occurs only at very low temperatures. This is the reason why the solidified RG are called cryogenic crystals. The centrosymmetric cubic close pack (ccp) structure is favored in RG due to the modification of the long-range Van der Waals force by the overlap of atomic excited

Chemical property	He	Ne	Ar	Kr	Xe
Atomic weight mean A	4.002	20.180	39.948	83,798	131,29
Atomic number Z	4	10	18	36	54
Melting temperature T_m (K)	–	24.56	83.81	115.78	161.40
Boiling temperature T_b (K)	4.22	27.10	87.30	119.93	165.05
gas density @ 298K ρ(g/l)	0.18	0.9 0	1.78	3.75	5.89
gas density @ T_b ρ(g/l)	16.6	9.56	5.77	8.89	9.99
liquid density @ T_b ρ(g/cm^3)	0.12	1,21	1.39	2.42	2.94
liquid density @ T_m ρ(g/cm^3)	–	1.25	1.41	2.45	3.08
solid density @ T_m ρ(g/cm^3)	–	1.44	1.62	2.83	3.54
Energy gap in liquid E_{gap} (eV)	19.8	–	13.4	11.55	11.67
Electron mobility in liquid μ_e (cm^2/(Vs))	–	$1.6{\cdot}10^{-3}$[*]	475	1800	2950
MIP energy loss in liquid $\frac{\partial E}{\partial x}$(MeV/cm)	0.23	2.04	2.105	3.28	3.7
Light Yield in liquid LY_{liquid} (γ/keV)	–	7	40	25	46

Table 1. Principal properties of rare gases. T_m and T_b are at 1 bar. Data from references [10]. [*] This value refers to the mobility of the "electron-bubble". The bubble is a macroscopic void that surrounds electron in liquid neon.

states with the neighboring atoms in the crystal [11]. This ccp structure is shown in figure 1. In this structure the lattice is a face centered cube with an RG atom at each lattice vertex. The lattice parameter (a) for the main RG solid crystals is presented in the table 2.

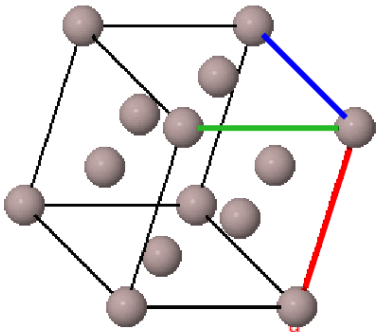

Figure 1. Sketch of the ccp structure with the three crystallographic orientations shown by red, green and blue axes.

	Ne	Ar	Kr	Xe
a (Å)	4.43	5.26	5.72	6.20

Table 2. Lattice parameter a of RG crystals.

2.2 Detection scheme

The detection scheme proposed in pure RG crystals is based on the direct ionization of the rare gas atoms when the incident particle, as for instance a DM particle, scatters with the target nucleus of the RG atom. The process of energy loss in RG was laid out by Lindhard et al. [12] and then discussed by others authors [13]. Experimentally, the efficiency of the ionization process is often expressed as charge yield and has been investigated and measured in liquid RGs in the past years [14]. Unfortunately, only sporadic studies regarding the temperature dependence of this parameter are present in literature. In the proposed scheme, electrons that are released according to the ionization process can drift under an electric field toward the crystal surface. Finally, they can be extracted and then collected into suitable in-vacuum sensors characterized by a high sensitivity and a low background.

3 Procedure and experimental set-up

To demonstrate the feasibility of the proposed detection scheme, we initially grew a large solid crystal of xenon and we measured the electrons' drift within the crystal itself. The experimental set-up and the procedure will be discussed in the next paragraphs.

3.1 Bridgman-Stockbarger modified technique

The idea at the basis of the Bridgman-Stockbarger (BS) technique is the slow solidification of the melt phase. This happens by translating the hot liquid zone in the direction of growing while a solid crystal is progressively formed behind the liquid. The chamber is filled with the liquid material at a temperature just above the temperature of melting. Starting from the bottom part of the container, where a crystal seed is located, the temperature is slowly lowered at a certain rate, typically of the order of 1 K/hour. In such a way, a temperature gradient is formed along the vertical direction, which is the direction of growing. The seed is a piece of single crystal and it ensures a single crystal growth along a certain crystallographic orientation. Also the temperature gradient need to be fixed at about $1 - 2$ K/cm. Lowering the temperature, while maintaining a fixed gradient, the portion of the container below the solidification temperature increases, and a large crystal is progressively formed. For the growth of RG solids the BS method is opportunely modified to operate at cryogenic temperatures and it is also named liquid-freezing or gradient-freezing technique [15].

3.2 Cryogenic chamber

We designed and built an apparatus composed by a pyrex chamber, a cryogenic vessel and a feedback temperature controller which are necessary for the growth of large xenon crystals following the Bridgman-Stockbarger modified technique. A gas purification system, described in a previous work [16], has also been used to purify the RG before the growing procedure. A dedicated electronic chain and high voltage power supplies have also been developed for charge detection.

Since pyrex is a very fragile material, especially when it is cooled at cryogenic temperatures, we adopted a custom-made chamber in which the junction between the glass and the stainless-steel flange is made of kovar. This metallic alloy ensures a good contact between the surfaces without outgassing; furthermore it has the same thermal expansion coefficient of pyrex making thus possible

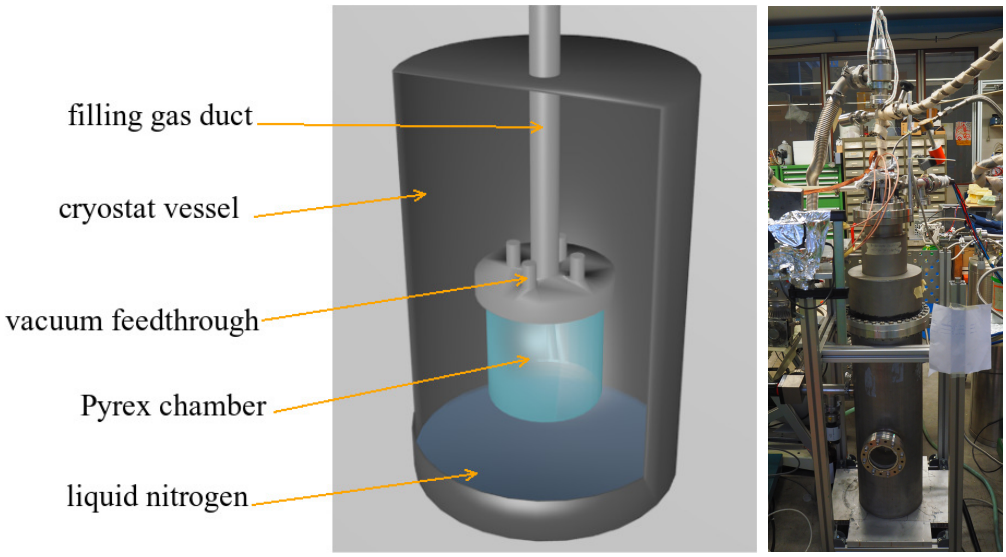

Figure 2. Sketch of the pyrex chamber enclosed inside a large stainless-steel cryostat that contains also liquid nitrogen. The picture on the right shows the large vessel that contains liquid nitrogen and where the pyrex chamber can be inserted.

the cooling of the chamber without cracking. The pyrex chamber has a cylindrical shape with a semi-spherical bottom. The internal diameter is 63 mm, the total length is 120 mm and the pyrex thickness is 1.5 mm. The chamber is mounted on a DN 63CF stainless-steel flange which is attached to a 1.5 m long tube that exits from the cryogenic vessel and it is connected to the gas purification system. Also a vacuum system and a pressure meter are connected to the chamber, as shown in figure 2.

The inner part of the pyrex chamber hosts the electrodes for the measurement of the drift of electrons inside the xenon crystal. A dedicated mechanical structure, as shown in figure 3, has been designed for this purpose. On the top flange of the chamber, three plastic (PEEK) columns hold the electrodes which are interlaced by small ceramic (macor) supports. The cathode is a 25 mm diameter disk mounted at the bottom at a distance of 18 mm from the base of the chamber. Placed about 18 mm above, the 25 mm diameter anode is the last electrode. A 21 mm inner diameter guard ring placed between them ensures the homogeneity of the electric field. Finally, at a distance of 3 mm from the anode, we mounted a 97% transmittance copper grid. Anode and cathode delimit a drift volume of about 21 cm^3 while, due to mechanical reasons in this prototype, the total available volume for the xenon growing, which is given by the chamber dimensions, is about 150 cm^3. Three different high-voltage power supplies provide the voltages at the electrodes, which are set as follow:

- anode potential: ground
- grid potential: −520 V
- guard-ring potential: −1000 V
- cathode potential: −1500 V

In such a way the electric field in the drift region is ~ 500 V/cm. A 2-dim simulation of the electric field amplitude and of the potential lines is shown in figure 3, on the right.

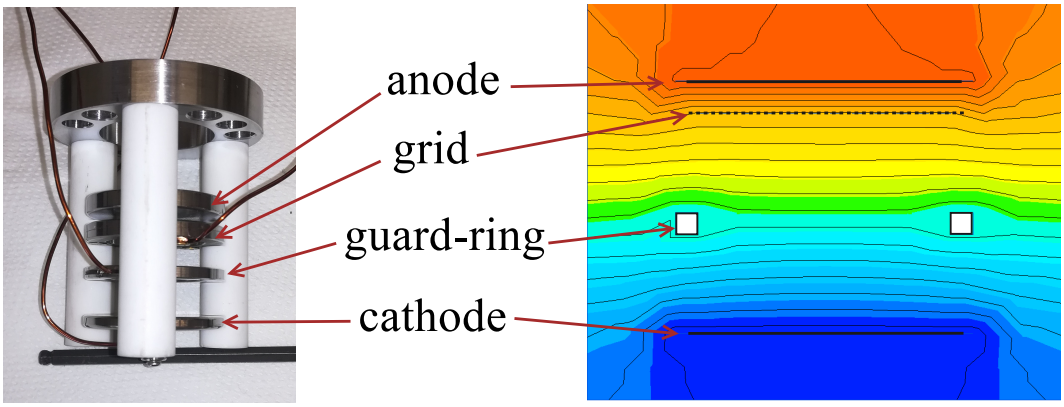

Figure 3. Left: picture of the inner part of the pyrex chamber with the macor holder for the electrodes. Right: simulation of the electric field inside the pyrex chamber. Colors correspond to different electric field: blue stands for ~ 0.5 V/cm while red for 1.6 kV/cm. Equipotential lines are also shown.

As shown in the picture of figure 2, the pyrex chamber is surrounded by the vapor of liquid nitrogen (LN_2), which is contained into a large cryogenic vessel equipped with two optical ports in the correspondence of the pyrex chamber. The liquid nitrogen is continuously refilled into the vessel using a small copper duct and the distance between the bottom part of the pyrex chamber and the LN_2 is maintained at 4 cm. Due to the cryogenic vapor, the chamber's wall reaches a temperature of ~ 90 K.

The temperature gradient has to be set precisely along the direction of growing in order to obtain a good crystal. Since the pyrex thermal conductivity at 150 K is roughly 1 $Wm^{-1}K^{-1}$, we decided to fix the temperature T_{set} along the vertical direction of the chamber with a step of 1 cm. For this reason, wire resistors with $R_{wire} \approx 1\,\Omega$ are glued to the pyrex external wall in the suitable point. Next to each wire, a calibrated platinum resistive temperature sensor (PT100) measures the local temperature T_{act}. In total, we mounted four resistive wires and five temperature sensors. An electronic module that can be interfaced at the PC through an USB port was also developed to simultaneously measure the value of each temperature sensor. The temperature along the pyrex chamber can be set and monitored through a custom Labview program specifically developed. This program is based on an active feedback system that exploits every temperature sensor and the associated resistive wire.

3.3 Growing procedure

In order to obtain a good optical quality and transparent solid [17, 18], the crystal growth was operated very slowly. Initially, the ~ 150 cm^3 pyrex chamber have been filled with about 460 grams of liquid xenon at 163 K. The Xe was previously purified in the gas purification set-up which is composed of an Oxysorb filter and a hot getter through a procedure described in a previous work [19]. Following the Bridgman-Stockbarger modified growing method, a temperature gradient $\nabla T = 1$ K/cm was applied at the pyrex chamber along the vertical direction. Thus, the bottom of the chamber was initially at 161 K, which is sufficient to start the formation of a crystal seed. The

process of crystal growth begins when the temperature gradient is progressively "moved" along the vertical direction. Due to the relatively large dimensions of the chamber, the optimal velocity is $\approx$ 1 K/hour. In such a way, the growing speed at the wall side is almost equal to the speed in the center and this ensures a flat growing surface. This velocity means that every hour each set-point temperature (T_{set}) is lowered by 1 K. Under these conditions the solid xenon grows almost uniformly and homogeneously over the 6 cm diameter, 10 cm long chamber.

4 Tests and measurements

After the crystal growth, we kept the solid xenon at about 153 K during the preliminary measurement regarding the detection of cosmic rays. When comic rays, mostly muons, pass through the xenon, they release energy in the crystal. The muon interaction with nucleus of xenon leads to the ionization and to the subsequent production of free electrons into the crystal. Due to the electric field, those electrons can drift within the solid and reach the anode, which is connected to a 1mV/fC gain charge amplifier (CA) with a time constant of 80 μs. Also the grid is connected to a similar CA with a different time constant (20 μs) to discriminate possible fake signals. The outputs of the CAs are read with an oscilloscope. We acquired signals for about 30 minutes, whereupon the energy spectrum is reconstructed and fitted using a Landau distribution. Figure 4 shows the obtained results. Due to the length (l) of ~18 mm of the fiducial volume in the chamber, a mean energy release of $\partial E/\partial x \cdot l \approx 6.6$ MeV is expected. Furthermore, the rate of incident cosmic muon is well established in literature [20]. The reduced chi-squared is $\chi^2/\mathrm{dof} = 2$, the maximum of the distribution is 6.3 ± 0.2 MeV and the measured rate of 3.8 events/4.1 $\mathrm{cm}^2\mathrm{min} \approx 0.93\,\mathrm{cm}^{-2}\mathrm{min}^{-1}$ is very close to the expected rate. Good agreement can thus be found comparing measured and expected values.

5 Conclusions

Many tests have been done in order to acquire the knowledge and the competences necessary to grow a large solid crystal of xenon exploiting the Bridgman-Stockbarger modified technique. The scalability study confirms the possibility to obtain a very large (kg-scale) single crystal of rare gas. This material represents the starting point for a possible development of a particle detector based on rare gas solid crystal, as in the proposed scheme. Using a xenon crystal and the set-up based on copper electrodes embedded into the solid, we were able to detect an amount of charge of the order of $\approx$ 1 fC and thus track the cosmic rays interaction in the material. The optimal agreement between experimental data and theoretical calculations such as in the measurement of the charge deposited in the crystal by cosmic muons, ensures the high quality of the crystal. Since the signal is constant for long time, charge trapping can be considered negligible and consequently, impurity or cracking sites are roughly absent in the specimen we grew. This measurement is a first important test that gives a positive answer to the possibility of applying the proposed scheme in rare gas crystals in the field of particle detection. A low energy threshold scheme can then be accomplished through the detection of a smaller number of electrons with suitable charge sensors such as microchannel plates or channeltron systems. In opportune conditions, these detectors are indeed characterized

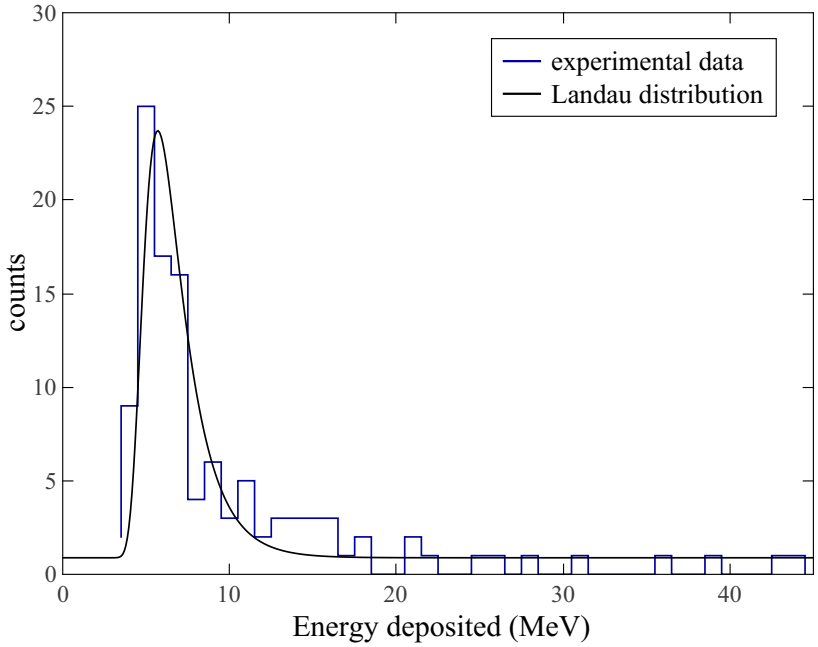

Figure 4. Energy spectrum of cosmic rays obtained from the signal obtain at the anode.

by a high efficiency and a low background. Studies in this way are needed and we are developing suitable experimental apparatuses to test the feasibility of this approach in more detail.

Moreover the use of the scheme above described, we also plan to grow RG crystals doped with alkali metals or rare earth atoms and exploit the internal energy level structure of these dopant materials. Combining these doped matrices with laser spectroscopy technique, and in particular with the laser induced ionization, we can in principle obtain a novel hybrid detection scheme characterized by a very low energy threshold as in the infrared quantum counter concept [21]. In such a scheme, the incident particle triggers the laser ionization process and thus an electron is released in the vacuum where it can be detected exploiting high efficiency single electron detectors [22].

Acknowledgments

Th work presented in this manuscript have been funded by the fifth scientific committee of INFN under AXIOMA and DEMIURGOS projects. Authors want to thank the precious technical work of E. Berto, F. Calaon, S. Marchini, M. Rebeschini, M. Tessaro and M. Zago.

References

[1] Aghanim, N. et al., *Planck 2018 results. VI. Cosmological parameters*, *arXiv:1807.06209*(2018).

[2] Bertone, G. and Tait, T.M.P., *A new era in the search for dark matter*, *Nat.* **562** (2018) 51.

[3] Feng, J.L., *Dark matter candidates from particle physics and methods of detection*, *Ann. Rev. Astron. Astr.* **48** (2010) 495–545.

[4] Bertone, G. and Hooper, D. and Silk, J., *Particle dark matter: evidence, candidates and constraints*, *Phys. Rep.* **405** (2005) 279–390.

[5] Zasov, A. et al., *Dark matter in galaxies*, *Phys.-Usp.* **60** (2017) 3.

[6] Peccei, R.D., *The strong CP problem and axions*, in M. Kuster et al. (Eds.) *Axions: Theory, Cosmology, and Experimental Searches, Lect. Notes Pys.***741** (Springer, Berlin Heidelberg 2008) 3–17.

[7] Pospelov, M. and Ritz, A. and Voloshin, M., *Secluded WIMP dark matter*, *Phy. Lett. B* **662** (2008) 53–61.

[8] Liu, J. and Chen, X. and Ji, X., *Current status of direct dark matter detection experiments*, *Nat. Phys.* **13** (2017) 212.

[9] Aprile, E.et al.,*Dark matter search results from a one ton-year exposure of XENON1T*, *Phys. Rev. Let.*, **121** (2018) 111302.

[10] Haynes, W.M., *CRC handbook of chemistry and physics*, *CRC press* (2014).

[11] Niebel, K.F. and Venables, J.A., *An explanation of the crystal structure of the rare gas solids*, *Proc. R. Soc. Lon. Ser.-A* **336** (1974) 365–377.

[12] Lindhard, J. and Scharff, M. and Schiott, H.E., *Range concepts and heavy ion ranges*, *Munksgaard Copenhagen, 1963*

[13] Chepel, Vitaly and Araujo, Henrique, *Liquid noble gas detectors for low energy particle physics*, *J. Instrum.*, **8** (2013) R04001

[14] Aprile, E. and Bolotnikov, A. E and Bolozdynya, A. I and Doke, T., *Noble gas detectors*, *John Wiley & Sons 2006*

[15] Klein, M.L. and Venables, J.A.*Rare gas solidsAcademic Press* **1** (1976)

[16] Feng, J.L., *Experimental setup for the growth of solid crystals of inert gases for particle detection*, *Rev. Sci. Instrum.* **88** (2017) 113303.

[17] Scheel, H.J., *The development of crystal growth technology*, *Cryst. Res. Technol.* (2003) 3–14.

[18] Yoo, J. et al., *Scalability study of solid xenon*, *J. Instrum.* **10** (2015) 04009.

[19] Carugno, G. et al., *A large liquid xenon time projection chamber for the study of the radiative pion decay*, *Nucl. Instrum. Meth. Phys. Res. A* **376** (1996) 149–154.

[20] Tanabashi, M. et al., *Review of particle physics*, *Phys. Rev. D* **98** (2018) 030001.

[21] Braggio, C. et al., *Axion dark matter detection by laser induced fluorescence in rare-earth doped materials* , *Sci. Rep.* **7** (2017) 15168.

[22] Guarise, M. et al., *Particle detection in rare gas solids: DEMIURGOS experiment*, *Nucl. Instrum. Methods Phys. Res. A* (2019) 162434.